

# KV PREDICTION FOR IMPROVED TIME TO FIRST TOKEN

Maxwell Horton\*, Qingqing Cao, Chenfan Sun, Yanzi Jin, Sachin Mehta†, Mohammad Rastegari†, & Moin Nabi  
Apple

## ABSTRACT

Inference with transformer models begins with a prompt processing step. This prompt processing step can be computationally expensive, taking up to 10s of seconds for billion-parameter models on edge devices. This introduces significant latency for the end user. To reduce the time spent producing the first output (known as the “time to first token”, or *TTFT*) of a pretrained model, we introduce a novel method called KV Prediction. In our method, a small *auxiliary* model is used to process the prompt and produce an approximation of the KV cache used by a *base* model. This approximated KV cache is then used with the base model for autoregressive generation without the need to query the auxiliary model again. Our method produces a pareto-optimal efficiency-accuracy trade-off when compared to baselines. On TriviaQA, we demonstrate relative accuracy improvements in the range of 15%–50% across a range of TTFT FLOPs budgets. We also demonstrate accuracy improvements of up to 30% on HumanEval python code completion. Additionally, we benchmark models on an Apple M2 Pro CPU and demonstrate that our improvement in FLOPs translates to a TTFT speedup on hardware. We release our code at <https://github.com/apple/corenet/tree/main/projects/kv-prediction>.

## 1 INTRODUCTION

Large language models (LLMs) have demonstrated impressive capabilities on many downstream tasks (Gunter et al., 2024; Achiam et al., 2023; Chowdhery et al., 2022; Abdin et al., 2024). However, the high computational cost of running large language models results in limited capabilities for on-device inference. On-device inference is essential for privacy, latency, energy efficiency, and performance in limited-connectivity areas (Frantar et al., 2022; Alizadeh-Vahid et al., 2023; Stojkovic et al., 2024). For these reasons, LLM efficiency remains an important and active area of research.

LLM inference with the popular transformer (Vaswani et al., 2017) architecture begins with a *prompt processing* phase, after which the model can begin streaming output tokens. The “time to first token” (TTFT) refers to the time taken to process the prompt and emit the first output token. In scenarios such as chatting with a user, the TTFT may be a more important runtime experience metric than autoregressive generation time, since the user can begin consuming outputs after the first token is produced. For on-device models, prompt processing times can be intolerably slow (up to 10s of seconds, Fig. 1). Reducing TTFT in these cases enables a better user experience.

We present a method to improve TTFT by processing the prompt with a small *auxiliary* transformer model. Our method runs the auxiliary model and stores its KV cache. It then uses a learned linear projection to predict the KV cache of another transformer model (the *base* model) using only the KV cache of the auxiliary model as input. Our method improves upon the efficiency-accuracy trade-off achievable by our baselines. For example, we demonstrate accuracy improvements of 15%–50% on question answering with TriviaQA (Joshi et al., 2017), and up to 30% on code completion with HumanEval (Chen et al., 2021) at fixed TTFT FLOP counts. We provide on-device timing experiments to demonstrate that our FLOPs gains translate to on-device runtime improvements.

\*Correspondence to [mhorton@apple.com](mailto:mhorton@apple.com).

†Work done at Apple. Now at Meta.

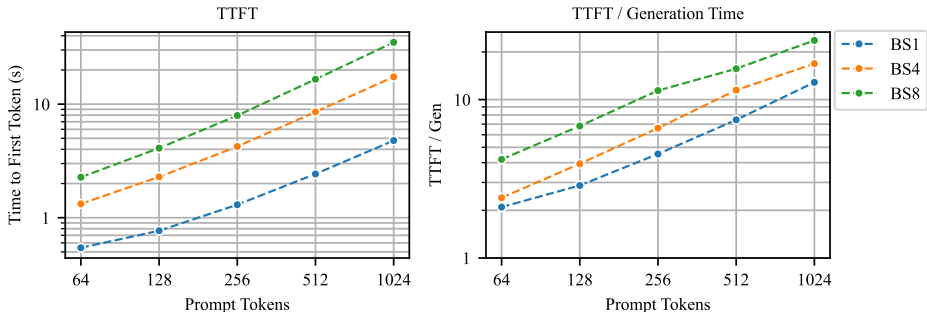


Figure 1: TTFT and ratio of TTFT to the time for a step of generation for an OpenELM 3B model on an M2 Pro CPU (EveryMac, 2024) with 32GB of RAM. We evaluate at batch sizes 1, 4, and 8.

Our contributions are as follows: (1) We develop a novel method called KV Prediction for improving on-device TTFT. (2) Our method produces a stronger efficiency-accuracy trade-off than baselines. (3) We analyze the runtime characteristics of KV Prediction models on-device. Additionally, we release our code for reproducibility at <https://github.com/apple/corenet/tree/main/projects/kv-prediction>.

## 2 RELATED WORK

**On-Device TTFT Efficiency:** Few works have explored our problem domain of improving on-device TTFT. LazyLLM (Fu et al., 2024) uses an attention-based token dropping strategy to drop unneeded tokens at inference time. These tokens can be revived later during the generation phase. Random token dropping (Yao et al., 2022) and static token pruning are both studied in Fu et al. (2024) as methods for improving TTFT. These methods are our baselines.

**Server-Side TTFT Efficiency:** Cachegen (Liu et al., 2023) compresses KV caches for faster TTFT, but their setup assumes that a precomputed, pre-compressed KV cache is stored on a server that is available over network. Other related works explore techniques for server-side TTFT efficiency (Agrawal et al., 2023; Lv et al., 2024; Agrawal et al., 2024) or long-context execution (which is currently not feasible on edge devices) (Gao et al., 2024; Jiang et al., 2024; Xiong et al., 2023). Our investigation differs from these in that we focus on on-device TTFT improvements.

**Context Compression:** Previous works have investigated compressing the KV cache for improving generation efficiency. PyramidKV (Cai et al., 2024), StreamingLLM (Xiao et al., 2023), SnapKV (Li et al., 2024), and Model Tells You What To Discard (Ge et al., 2023) all compress the KV cache along the token dimension by observing attention scores and pruning irrelevant tokens. However, their methods compute a forward pass before pruning. Thus, they improve generation time, but not TTFT. Layer-Condensed KV Cache (Wu & Tu, 2024) compresses an  $N$ -layer KV cache into a 1-layer KV cache, but requires 9 prompt processing steps and negatively impacts TTFT. Other works such as KIVI (Liu et al., 2024) and GEAR (Kang et al., 2024) have explored quantizing the KV cache, but do not improve TTFT.

**General Techniques for Efficiency:** Many works have explored quantization (Lin et al., 2023; Tseng et al., 2024; Frantar et al., 2022; Dettmers et al., 2023; Shao et al., 2023; Egiazarian et al., 2024), pruning (Alizadeh-Vahid et al., 2023; Ma et al., 2023; Zheng et al., 2024), and efficient design (Mehta et al., 2024; Zhang et al., 2024; Abdin et al., 2024) to improve LLM efficiency. These techniques are orthogonal to ours, as they can be combined with our method or our baselines.

## 3 KV PREDICTION

Recent work has shown that the KV cache can be compressed with little or no loss in accuracy at generation time (Cai et al., 2024; Li et al., 2024; Xiao et al., 2023; Ge et al., 2023). We hypothesize that the KV cache for a model can be approximated efficiently to reduce on-device TTFT. We use a

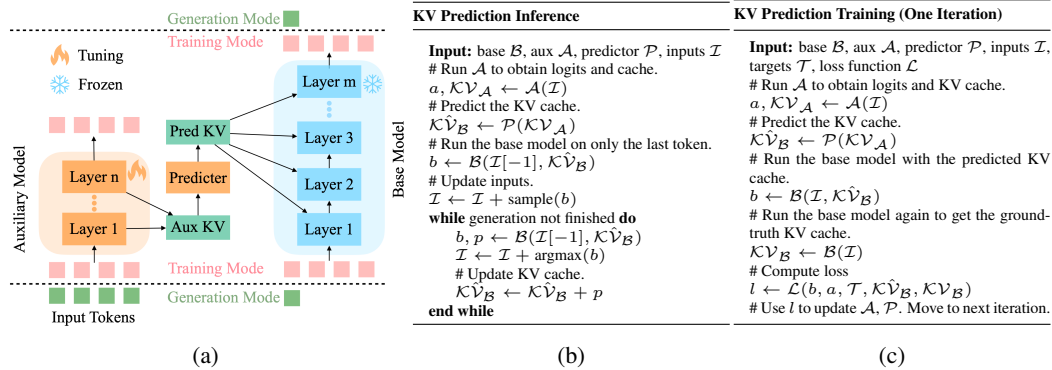


Figure 2: (a) An overview of our method. (b) Our inference method. (c) Our training method.

smaller auxiliary transformer to process the prompt. Then, a set of learned linear projections is used to predict the base model’s KV cache using the auxiliary model’s KV cache (Fig. 2a).

### 3.1 PREDICTING KV CACHES

Our model contains a frozen pretrained base network  $\mathcal{B}$ , a learned auxiliary network  $\mathcal{A}$ , and a learned KV predictor  $\mathcal{P}$ . The auxiliary and predictor networks are used to generate the predicted KV cache efficiently. Afterwards, inference proceeds with only the base model.

**Inference:** During inference (Fig. 2b) the prompt is passed to the auxiliary model and the auxiliary KV cache  $\mathcal{KV}_{\mathcal{A}}$  is computed. Then, the predicted base KV cache  $\mathcal{KV}_{\hat{\mathcal{B}}} = \mathcal{P}(\mathcal{KV}_{\mathcal{A}})$  is computed. At this point,  $\mathcal{A}$  and  $\mathcal{P}$  are no longer required to continue inference. To generate the first token, a single-token generation step of  $\mathcal{B}$  is run, but with  $\mathcal{KV}_{\hat{\mathcal{B}}}$  being used as the keys and values in the attention operations (instead of using the base model’s QKV projections). The logits produced from this step are used to produce the first token. Afterwards, standard autoregressive inference is used.

**Training:** During training (Fig. 2c), a sequence of tokens  $\mathcal{I}$  are fed to the auxiliary model  $\mathcal{A}$  to produce output logits  $\mathcal{A}(\mathcal{I})$  and a KV cache  $\mathcal{KV}_{\mathcal{A}}$ . Then, the predicted KV cache  $\mathcal{KV}_{\hat{\mathcal{B}}} = \mathcal{P}(\mathcal{KV}_{\mathcal{A}})$  is computed. Finally, a forward pass of  $\mathcal{B}$  is computed using the predicted KV cache  $\mathcal{KV}_{\hat{\mathcal{B}}}$  (instead of using the keys and values from the base model’s QKV projections) to produce output logits  $\mathcal{B}(\mathcal{I})$ . See Appendix A for details on our loss function.

### 3.2 ARCHITECTURAL DETAILS

Our KV Prediction models are fully specified by our base, auxiliary, and predictor networks. Our base network always consists of a standard pretrained frozen transformer network.

**Auxiliary Networks:** We use two different methods for choosing an auxiliary network. In the first method, referred to as KVP-C (KV Prediction with a Canonical model), we choose the auxiliary network to be a smaller model in the same family as the base model. In the second method for choosing an auxiliary network, referred to as KVP-LP (KV Prediction with a Layer-Pruned model), our auxiliary network consists of a copy of the base network with some of the layers removed.

**Predictor Networks:** For our *predictor* network, we use a set of learned linear transforms to predict each layer of the base model’s KV cache independently. Each transform takes in one layer of the auxiliary KV cache and predicts one layer of the base KV cache. See Appendix C for details.

**Model Specification:** When experimenting with KV Prediction, we use OpenELM (Mehta et al., 2024) models. For KVP-C experiments, we use smaller models from the OpenELM family as the auxiliary models. For KVP-LP experiments, we define a set of layer-pruned OpenELM models in Appendix B, which we use as the auxiliary model. When referring to a KV prediction architecture, we specify its base network, followed by either KVP-C or KVP-LP, followed by its auxiliary network (e.g. OE1.1B-KVP-C-450M). See Appendix C for a detailed table listing the base, auxiliary, and predictor settings for all models used for experimentation.

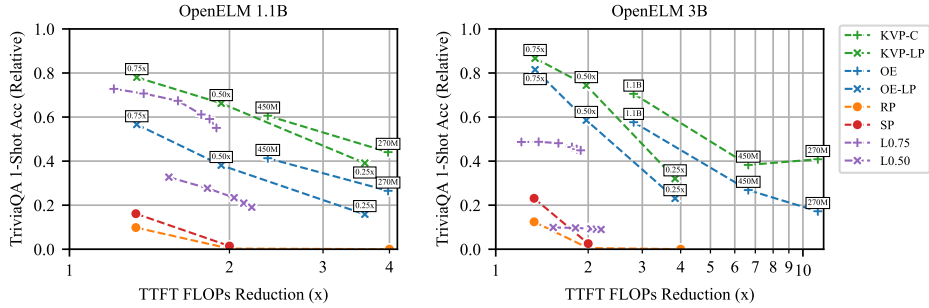


Figure 3: TriviaQA results. The x-axis shows the relative reduction in FLOPs compared to the base network, and the y-axis shows the relative accuracy retention compared to the base network. For KV Prediction models (green), points are annotated with the auxiliary network used. For OpenELM baselines (blue), points are annotated with the OpenELM variant used. (Left): Using a base network of OpenELM 1.1B for KV Prediction. (Right): Using a base network of OpenELM 3B.

### 3.3 RUNTIME ANALYSIS

**FLOPs:** We analyze the improvement in TTFT of our method. The FLOPs-per-token compute cost of transformers inference can be estimated as  $2P$ , where  $P$  is the number of parameters in the model (Kaplan et al., 2020). The total FLOPs required for prompt processing for  $N$  tokens is  $NP$ . Thus, the ratio of the FLOPs of prompt processing to the ratio of FLOPs for a single generation step is  $N$ .

Let  $t_{\mathcal{N}}(N)$  denote the forward pass FLOPs of network  $\mathcal{N}$  with  $N$  input tokens. As described in Section 3, producing the first output token using KV Prediction requires an  $N$ -token forward pass of  $\mathcal{A}$ , followed by an  $N$ -token forward pass of  $\mathcal{P}$ , then a single-token forward pass of  $\mathcal{B}$  (to generate the first output token using the predicted KV cache). The FLOPs taken to process the prompt and generate the first token is  $t_{\mathcal{A}}(N) + t_{\mathcal{P}}(N) + t_{\mathcal{B}}(1) = Nt_{\mathcal{A}}(1) + t_{\mathcal{P}}(N) + t_{\mathcal{B}}(1)$ . The computational cost of  $t_{\mathcal{P}}(N)$  is negligible compared to  $Nt_{\mathcal{A}}(1)$ , as it contains only a linear layer of smaller dimensionality than the transformer’s FFN layers (corresponding to an overhead of roughly 1% of the FLOPs of the auxiliary network). For sufficient  $N$ ,  $Nt_{\mathcal{A}}(1) \gg t_{\mathcal{B}}(1)$ , and the FLOPs of a single inference are dominated by  $Nt_{\mathcal{A}}(1)$ . Thus, the relative improvement in prompt processing FLOPs over the standard inference setup can be approximated as  $t_{\mathcal{A}}(1)/t_{\mathcal{B}}(1)$ .

**Memory Usage:** Our method requires deploying an auxiliary and predictor network in addition to the base network. The predictor is much smaller than a single transformer block, thus occupies negligible memory. The auxiliary network is generally a fraction of the size of the base network. Additionally, the auxiliary network can be unloaded from memory after prompt processing, as it is not needed during generation. To avoid cold starts on the next query, the auxiliary model can be reloaded into memory after inference. We do not employ this optimization in timing experiments.

## 4 EXPERIMENTAL SETUP

We experiment with KV Prediction using OpenELM (Mehta et al., 2024). To train our models, we reload the base and auxiliary model weights from pretrained OpenELM models. We follow the training hyperparameters of OpenELM, training on RefinedWeb (Penedo et al., 2023), ArXiv (Clement et al., 2019), and Wikipedia (Foundation, 2024). For code completion experiments, we train on The Stack (Kocetkov et al., 2022). See Appendix D for additional details.

**Baselines:** Our first set of baselines uses token dropping. We use random token pruning (**RP**) and static token pruning (**SP**) at various token retention rates. Our LazyLLM (Fu et al., 2024) baselines have a starting retention rate of 0.75 (**L0.75**) and 0.50 (**L0.50**). We sweep across ending retention rates to produce an efficiency-accuracy trade-off. See Appendix E for more details.

Our second set of baselines sweeps across model sizes in the OpenELM family. Our **OE** baseline consists of OpenELM 1.1B, OpenELM450M, and OpenELM270M. Our **OE-LP** baseline consists of OpenELM layer-pruned models, fine-tuned with the same settings as our KV Prediction models.

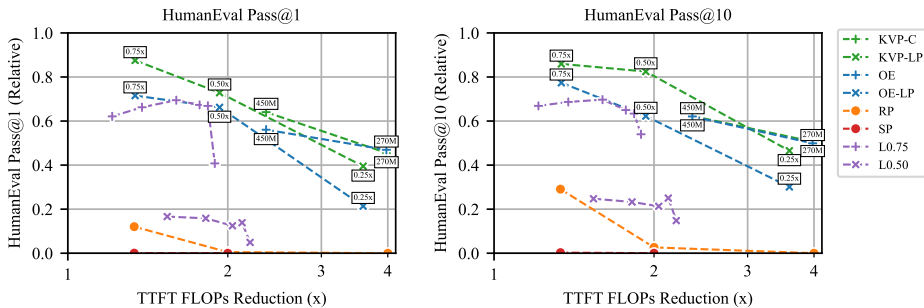


Figure 4: Efficiency-accuracy trade-off of our KV Prediction method (KVP-C, KVP-LP) compared to baselines on HumanEval python code completion. The x-axis shows the relative speedup in FLOPs compared to OpenELM 1.1B, and the y-axis shows the relative accuracy retention compared to OpenELM 1.1B. (Left): HumanEval Pass@1. (Right): HumanEval Pass@10.

## 5 RESULTS

Here, we empirically analyze our method. In Section 5.1, we demonstrate that our model improves the pareto-optimal efficiency-accuracy trade-off on TriviaQA (Joshi et al., 2017). In Section 5.2, we demonstrate that our model also achieves the pareto-optimal efficiency-accuracy tradeoff on python code completion with HumanEval (Chen et al., 2021). In Section 5.3, we analyze the on-device runtime improvement in TTFT, demonstrating that our theoretical FLOPs reduction translates to runtime improvement on real hardware.

### 5.1 QUESTION-ANSWERING ON TRIVIAQA

We investigate our method’s efficiency-accuracy trade-off for OpenELM 1.1B and OpenELM 3B in Fig. 3 (we also present these results in table format in Appendix F). We measure accuracy on TriviaQA using LLM Eval Harness (Gao et al., 2021). Our method produces the strongest efficiency-accuracy trade-off, tracing a pareto-optimal curve. The KVP-C strategy outperforms the KVP-LP method, but the KVP-LP method can achieve higher accuracy retention.

Our OE baselines correspond to only using the auxiliary model architecture from the KVP-C experiment (but with different weights). Directly comparing our KVP-C method to these baselines, we see that our method strongly increases accuracy. The same observation holds for OE-LP baselines and KVP-LP models. Random pruning (RP) and static pruning (SP) do not perform well. We conjecture that these methods are better suited to long-context scenarios with redundant tokens. For example, in Fu et al. (2024), these methods are shown to perform well on long-context problems such as multi-document question answering.

### 5.2 CODE COMPLETION RESULTS

We investigate our method’s efficacy for code completion with a base model of OpenELM 1.1B in Fig. 4 (we also present these results in table format in Appendix F). We train our models on the Stack and measure performance on HumanEval’s python code completion benchmark.

We find that our model produces the strongest efficiency-accuracy trade-off, tracing a pareto-optimal curve. As in the case of TriviaQA, our KVP-C strategy outperforms the KVP-LP method, but the KVP-LP method is able to achieve a higher accuracy retention because larger models can be chosen.

Our method obtains a much stronger efficiency-accuracy trade-off than OE and OE-LP baselines. Our KV prediction method also improves over token-pruning baselines (RP, SP, L0.75, and L0.50) in terms of efficiency and accuracy. We find that random pruning and static pruning do not perform well on HumanEval, which has queries of  $\sim 100$  tokens. In Fu et al. (2024), these baselines are shown to be more competitive on longer code samples.

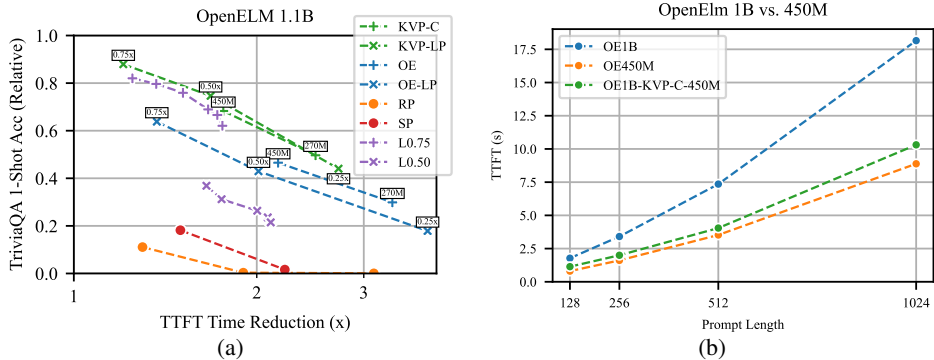


Figure 5: (Fig. 5a): Accuracy on the TriviaQA dataset compared to benchmarked time to first token on CPU. (Fig. 5b): The time to first token of our KVP prediction model OE1.1B-KVP-C-450M compared to OpenELM 1.1B and OpenELM450M.

### 5.3 TIMING EXPERIMENTS

We perform timing experiments to analyze the TTFT improvement of our method. See Appendix G for experimental details. We plot the relative TTFT reduction and the accuracy retention in Fig. 5a. Our method traces the pareto-optimal frontier. See Appendix F for results in table format.

Next, we measure the TTFT of a KV Prediction model (OE1.1B-KVP-C-450M) compared to its base (OpenELM 1.1B) and auxiliary (OpenELM 450M) models (Fig. 5b). The TTFT of OE1.1B-KVP-C-450M nearly matches the TTFT of its auxiliary model, demonstrating that KV prediction has a small overhead on-device relative to only running the auxiliary model (while demonstrating strong accuracy advantages over only running the auxiliary model, as discussed in Section 5.1 and Section 5.2).

## 6 ANALYSIS

We present additional analysis in Appendix H. We analyze the performance on multiple-choice question-answering, as well as the error in cache predictions made by the predictor network.

## 7 CONCLUSION

We present a method for improving time to first token (TTFT) called KV Prediction. Our method uses a small auxiliary model to efficiently predict the KV cache needed by a larger base model. We analyze the theoretical and actual speedup of our model, as well as the accuracy retention. We find that our model maintains a strong efficiency-accuracy trade-off, creating a pareto-optimal trade-off in terms of accuracy retention and TTFT.

## 8 ACKNOWLEDGMENTS

We would like to thank Colorado Reed, Alvin Wan, Binazir Karimzadeh, Mengxia Yu, Christian Koguchi, Qi Shan, Rasoul Shafipour, Minsik Cho, Mahyar Najibi, Mehrdad Farajtabar and Qichen Fu for useful discussions and valuable feedback.

## REFERENCES

Marah Abdin, Sam Ade Jacobs, Ammar Ahmad Awan, Jyoti Aneja, Ahmed Awadallah, Hany Hassan Awadalla, Nguyen Bach, Amit Bahree, Arash Bakhtiari, Harkirat Singh Behl, Alon Benhaim, Misha Bilenko, Johan Bjorck, Sébastien Bubeck, Martin Cai, Caio Cesar Teodoro Mendes, Weizhu Chen, Vishrav Chaudhary, Parul Chopra, Allison Del Giorno, Gustavo de Rosa, Matthew Dixon, Ronen Eldan, Dan Iter, Abhishek Goswami, Suriya Gunasekar, Emman Haider, Junheng

Hao, Russell J. Hewett, Jamie Huynh, Mojan Javaheripi, Xin Jin, Piero Kauffmann, Nikos Karampatziakis, Dongwoo Kim, Young Jin Kim, Mahoud Khademi, Lev Kurilenko, James R. Lee, Yin Tat Lee, Yuanzhi Li, Chen Liang, Weishung Liu, Eric Lin, Zeqi Lin, Piyush Madan, Arindam Mitra, Hardik Modi, Anh Nguyen, Brandon Norick, Barun Patra, Daniel Perez-Becker, Thomas Portet, Reid Pryzant, Heyang Qin, Marko Radmilac, Corby Rosset, Sambudha Roy, Olli Saarikivi, Amin Saied, Adil Salim, Michael Santacrose, Shital Shah, Ning Shang, Hiteshi Sharma, Xianmin Song, Olatunji Ruwase, Xin Wang, Rachel Ward, Guanhua Wang, Philipp Witte, Michael Wyatt, Can Xu, Jiahang Xu, Sonali Yadav, Fan Yang, Ziyi Yang, Donghan Yu, Cheng-Yuan Zhang, Cyril Zhang, Jianwen Zhang, Li Lyna Zhang, Yi Zhang, Yunan Zhang, and Xiren Zhou. Phi-3 technical report: A highly capable language model locally on your phone. *ArXiv*, abs/2404.14219, 2024. URL <https://api.semanticscholar.org/CorpusID:269293048>.

OpenAI Josh Achiam, Steven Adler, Sandhini Agarwal, Lama Ahmad, Ilge Akkaya, Florencia Leoni Aleman, Diogo Almeida, Janko Altenschmidt, Sam Altman, Shyamal Anadkat, Red Avila, Igor Babuschkin, Suchir Balaji, Valerie Balcom, Paul Baltescu, Haiming Bao, Mo Bavarian, Jeff Belgum, Irwan Bello, Jake Berdine, Gabriel Bernadett-Shapiro, Christopher Berner, Lenny Bogdonoff, Oleg Boiko, Madelaine Boyd, Anna-Luisa Brakman, Greg Brockman, Tim Brooks, Miles Brundage, Kevin Button, Trevor Cai, Rosie Campbell, Andrew Cann, Brittany Carey, Chelsea Carlson, Rory Carmichael, Brooke Chan, Che Chang, Fotis Chantzis, Derek Chen, Sully Chen, Ruby Chen, Jason Chen, Mark Chen, Benjamin Chess, Chester Cho, Casey Chu, Hyung Won Chung, Dave Cummings, Jeremiah Currier, Yunxing Dai, Cory Decareaux, Thomas Degry, Noah Deutsch, Damien Deville, Arka Dhar, David Dohan, Steve Dowling, Sheila Dunning, Adrien Ecoffet, Atty Eleti, Tyna Eloundou, David Farhi, Liam Fedus, Niko Felix, Simón Posada Fishman, Juston Forte, Isabella Fulford, Leo Gao, Elie Georges, Christian Gibson, Vik Goel, Tarun Gogineni, Gabriel Goh, Raphael Gontijo-Lopes, Jonathan Gordon, Morgan Grafstein, Scott Gray, Ryan Greene, Joshua Gross, Shixiang Shane Gu, Yufei Guo, Chris Hallacy, Jesse Han, Jeff Harris, Yuchen He, Mike Heaton, Johannes Heidecke, Chris Hesse, Alan Hickey, Wade Hickey, Peter Hoeschele, Brandon Houghton, Kenny Hsu, Shengli Hu, Xin Hu, Joost Huizinga, Shantanu Jain, Shawn Jain, Joanne Jang, Angela Jiang, Roger Jiang, Haozhun Jin, Denny Jin, Shino Jomoto, Billie Jonn, Heewoo Jun, Tomer Kaftan, Lukasz Kaiser, Ali Kamali, Ingmar Kanitscheider, Nitish Shirish Keskar, Tabarak Khan, Logan Kilpatrick, Jong Wook Kim, Christina Kim, Yongjik Kim, Hendrik Kirchner, Jamie Ryan Kiros, Matthew Knight, Daniel Kokotajlo, Lukasz Kondraciuk, Andrew Kondrich, Aris Konstantinidis, Kyle Kosic, Gretchen Krueger, Vishal Kuo, Michael Lampe, Ikai Lan, Teddy Lee, Jan Leike, Jade Leung, Daniel Levy, Chak Ming Li, Rachel Lim, Molly Lin, Stephanie Lin, Mateusz Litwin, Theresa Lopez, Ryan Lowe, Patricia Lue, Anna Makanju, Kim Malfacini, Sam Manning, Todor Markov, Yaniv Markovski, Bianca Martin, Katie Mayer, Andrew Mayne, Bob McGrew, Scott Mayer McKinney, Christine McLeavey, Paul McMillan, Jake McNeil, David Medina, Aalok Mehta, Jacob Menick, Luke Metz, Andrey Mishchenko, Pamela Mishkin, Vinnie Monaco, Evan Morikawa, Daniel P. Mossing, Tong Mu, Mira Murati, Oleg Murk, David Mely, Ashvin Nair, Reiichiro Nakano, Rajeev Nayak, Arvind Neelakantan, Richard Ngo, Hyeonwoo Noh, Ouyang Long, Cullen O’Keefe, Jakub W. Pachocki, Alex Paino, Joe Palermo, Ashley Pantuliano, Giambattista Parascandolo, Joel Parish, Emy Parparita, Alexandre Passos, Mikhail Pavlov, Andrew Peng, Adam Perelman, Filipe de Avila Belbute Peres, Michael Petrov, Henrique Pondé de Oliveira Pinto, Michael Pokorny, Michelle Pokrass, Vitchyr H. Pong, Tolly Powell, Alethea Power, Boris Power, Elizabeth Proehl, Raul Puri, Alec Radford, Jack W. Rae, Aditya Ramesh, Cameron Raymond, Francis Real, Kendra Rimbach, Carl Ross, Bob Rotsted, Henri Roussez, Nick Ryder, Mario D. Saltarelli, Ted Sanders, Shibani Santurkar, Girish Sastry, Heather Schmidt, David Schnurr, John Schulman, Daniel Selsam, Kyla Sheppard, Toki Sherbakov, Jessica Shieh, Sarah Shoker, Pranav Shyam, Szymon Sidor, Eric Sigler, Maddie Simens, Jordan Sitkin, Katarina Slama, Ian Sohl, Benjamin D. Sokolowsky, Yang Song, Natalie Staudacher, Felipe Petroski Such, Natalie Summers, Ilya Sutskever, Jie Tang, Nikolas A. Tezak, Madeleine Thompson, Phil Tillet, Amin Tootoonchian, Elizabeth Tseng, Preston Tuggle, Nick Turley, Jerry Tworek, Juan Felipe Cerón Uribe, Andrea Vallone, Arun Vijayvergiya, Chelsea Voss, Carroll L. Wainwright, Justin Jay Wang, Alvin Wang, Ben Wang, Jonathan Ward, Jason Wei, CJ Weinmann, Akila Welihinda, Peter Welinder, Jiayi Weng, Lilian Weng, Matt Wiethoff, Dave Willner, Clemens Winter, Samuel Wolrich, Hannah Wong, Lauren Workman, Sherwin Wu, Jeff Wu, Michael Wu, Kai Xiao, Tao Xu, Sarah Yoo, Kevin Yu, Qiming Yuan, Wojciech Zaremba, Rowan Zellers, Chong Zhang, Marvin Zhang, Shengjia Zhao, Tianhao Zheng, Juntang Zhuang, William Zhuk, and Barret Zoph. Gpt-4 technical report. 2023. URL

<https://api.semanticscholar.org/CorpusID:257532815>.

Amey Agrawal, Ashish Panwar, Jayashree Mohan, Nipun Kwatra, Bhargav S. Gulavani, and Ramachandran Ramjee. Sarathi: Efficient llm inference by piggybacking decodes with chunked prefills. *ArXiv*, abs/2308.16369, 2023. URL <https://api.semanticscholar.org/CorpusID:261395577>.

Amey Agrawal, Anmol Agarwal, Nitin Kedia, Jayashree Mohan, Souvik Kundu, Nipun Kwatra, Ramachandran Ramjee, and Alexey Tumanov. Etalon: Holistic performance evaluation framework for llm inference systems, 2024. URL <https://arxiv.org/abs/2407.07000>.

Keivan Alizadeh-Vahid, Iman Mirzadeh, Dmitry Belenko, Karen Khatamifard, Minsik Cho, Carlo C. Del Mundo, Mohammad Rastegari, and Mehrdad Farajtabar. Llm in a flash: Efficient large language model inference with limited memory. *ArXiv*, abs/2312.11514, 2023. URL <https://api.semanticscholar.org/CorpusID:266362016>.

William Brandon, Mayank Mishra, Aniruddha Nrusimha, Rameswar Panda, and Jonathan Ragan-Kelley. Reducing transformer key-value cache size with cross-layer attention. *ArXiv*, abs/2405.12981, 2024. URL <https://api.semanticscholar.org/CorpusID:269930400>.

Zefan Cai, Yichi Zhang, Bofei Gao, Yuliang Liu, Tianyu Liu, Keming Lu, Wayne Xiong, Yue Dong, Baobao Chang, Junjie Hu, and Wen Xiao. Pyramidkv: Dynamic kv cache compression based on pyramidal information funneling. *ArXiv*, abs/2406.02069, 2024. URL <https://api.semanticscholar.org/CorpusID:270226243>.

Mark Chen, Jerry Tworek, Heewoo Jun, Qiming Yuan, Henrique Pondé, Jared Kaplan, Harrison Edwards, Yura Burda, Nicholas Joseph, Greg Brockman, Alex Ray, Raul Puri, Gretchen Krueger, Michael Petrov, Heidy Khlaaf, Girish Sastry, Pamela Mishkin, Brooke Chan, Scott Gray, Nick Ryder, Mikhail Pavlov, Alethea Power, Lukasz Kaiser, Mohammad Bavarian, Clemens Winter, Philippe Tillet, Felipe Petroski Such, David W. Cummings, Matthias Plappert, Fotios Chantzis, Elizabeth Barnes, Ariel Herbert-Voss, William H. Guss, Alex Nichol, Igor Babuschkin, Suchir Balaji, Shantanu Jain, Andrew Carr, Jan Leike, Joshua Achiam, Vedant Misra, Evan Morikawa, Alec Radford, Matthew M. Knight, Miles Brundage, Mira Murati, Katie Mayer, Peter Welinder, Bob McGrew, Dario Amodei, Sam McCandlish, Ilya Sutskever, and Wojciech Zaremba. Evaluating large language models trained on code. *ArXiv*, abs/2107.03374, 2021. URL <https://api.semanticscholar.org/CorpusID:235755472>.

Aakanksha Chowdhery, Sharan Narang, Jacob Devlin, Maarten Bosma, Gaurav Mishra, Adam Roberts, Paul Barham, Hyung Won Chung, Charles Sutton, Sebastian Gehrmann, Parker Schuh, Kensen Shi, Sasha Tsvyashchenko, Joshua Maynez, Abhishek Rao, Parker Barnes, Yi Tay, Noam M. Shazeer, Vinodkumar Prabhakaran, Emily Reif, Nan Du, Ben Hutchinson, Reiner Pope, James Bradbury, Jacob Austin, Michael Isard, Guy Gur-Ari, Pengcheng Yin, Toju Duke, Anselm Levskaya, Sanjay Ghemawat, Sunipa Dev, Henryk Michalewski, Xavier García, Vedant Misra, Kevin Robinson, Liam Fedus, Denny Zhou, Daphne Ippolito, David Luan, Hyeontaek Lim, Barret Zoph, Alexander Spiridonov, Ryan Sepassi, David Dohan, Shivani Agrawal, Mark Omernick, Andrew M. Dai, Thanumalayan Sankaranarayanan Pillai, Marie Pellat, Aitor Lewkowycz, Erica Moreira, Rewon Child, Oleksandr Polozov, Katherine Lee, Zongwei Zhou, Xuezhi Wang, Brennan Saeta, Mark Díaz, Orhan Firat, Michele Catasta, Jason Wei, Kathleen S. Meier-Hellstern, Douglas Eck, Jeff Dean, Slav Petrov, and Noah Fiedel. Palm: Scaling language modeling with pathways. *ArXiv*, abs/2204.02311, 2022. URL <https://api.semanticscholar.org/CorpusID:247951931>.

Colin B. Clement, Matthew Bierbaum, Kevin P. O’Keeffe, and Alexander A. Alemi. On the use of arxiv as a dataset, 2019.

Tim Dettmers, Ruslan Svirschevski, Vage Egiazarian, Denis Kuznedelev, Elias Frantar, Saleh Ashkboos, Alexander Borzunov, Torsten Hoefler, and Dan Alistarh. Spqr: A sparse-quantized representation for near-lossless llm weight compression. *ArXiv*, abs/2306.03078, 2023. URL <https://api.semanticscholar.org/CorpusID:259076379>.

- Vage Egiazarian, Andrei Panferov, Denis Kuznedelev, Elias Frantar, Artem Babenko, and Dan Alistarh. Extreme compression of large language models via additive quantization. *ArXiv*, abs/2401.06118, 2024. URL <https://api.semanticscholar.org/CorpusID:266933421>.
- EveryMac. Apple macbook pro "m2 pro" 12 cpu/19 gpu 16" specs. [https://everymac.com/systems/apple/macbook\\_pro/specs/macbook-pro-m2-pro-12-core-cpu-19-core-gpu-16-2023-specs.html](https://everymac.com/systems/apple/macbook_pro/specs/macbook-pro-m2-pro-12-core-cpu-19-core-gpu-16-2023-specs.html), 2024. Accessed: 2024-10-01.
- Wikimedia Foundation. Wikimedia downloads, 2024. URL <https://dumps.wikimedia.org>.
- Elias Frantar, Saleh Ashkboos, Torsten Hoefler, and Dan Alistarh. Gptq: Accurate post-training quantization for generative pre-trained transformers. *ArXiv*, abs/2210.17323, 2022. URL <https://api.semanticscholar.org/CorpusID:253237200>.
- Qichen Fu, Minsik Cho, Thomas Merth, Sachin Mehta, Mohammad Rastegari, and Mahyar Najibi. Lazyllm: Dynamic token pruning for efficient long context llm inference. 2024. URL <https://api.semanticscholar.org/CorpusID:271310096>.
- Leo Gao, Jonathan Tow, Stella Biderman, Sid Black, Anthony DiPofi, Charles Foster, Laurence Golding, Jeffrey Hsu, Kyle McDonell, Niklas Muennighoff, Jason Phang, Laria Reynolds, Eric Tang, Anish Thite, Ben Wang, Kevin Wang, and Andy Zou. A framework for few-shot language model evaluation, September 2021. URL <https://doi.org/10.5281/zenodo.5371628>.
- Yizhao Gao, Zhichen Zeng, Dayou Du, Shijie Cao, Hayden Kwok-Hay So, Ting Cao, Fan Yang, and Mao Yang. Seerattention: Learning intrinsic sparse attention in your llms. 2024. URL <https://api.semanticscholar.org/CorpusID:273403508>.
- Suyu Ge, Yunan Zhang, Liyuan Liu, Minjia Zhang, Jiawei Han, and Jianfeng Gao. Model tells you what to discard: Adaptive kv cache compression for llms. *ArXiv*, abs/2310.01801, 2023. URL <https://api.semanticscholar.org/CorpusID:263609075>.
- Tom Gunter, Zirui Wang, Chong Wang, Ruoming Pang, Andy Narayanan, Aonan Zhang, Bowen Zhang, Chen Chen, Chung-Cheng Chiu, David Qiu, Deepak Gopinath, Dian Ang Yap, Dong Yin, Feng Nan, Floris Weers, Guoli Yin, Haoshuo Huang, Jianyu Wang, Jiarui Lu, John Peebles, Kewei Ye, Mark Lee, Nan Du, Qibin Chen, Quentin Keunebroek, Sam Wiseman, Syd Evans, Tao Lei, Vivek Rathod, Xiang Kong, Xianzhi Du, Yanghao Li, Yongqiang Wang, Yuan Gao, Zaid Ahmed, Zhaoyang Xu, Zhiyun Lu, Al Rashid, Albin Madappally Jose, Alec Doane, Alfredo Bencomo, Allison Vanderby, Andrew Hansen, Ankur Jain, Anupama Mann Anupama, Areeba Kamal, Bugu Wu, Carolina Brum, Charlie Maalouf, Chinguun Erdenebileg, Chris Dulhanty, Dominik Moritz, Doug Kang, Eduardo Jimenez, Evan Ladd, Fang Shi, Felix Bai, Frank Chu, Fred Hohman, Hadas Koteck, Hannah Gillis Coleman, Jane Li, Jeffrey P. Bigham, Jeffery Cao, Jeff Lai, Jessica Cheung, Jiulong Shan, Joe Zhou, John Li, Jun Qin, Karanjeet Singh, Karla Vega, Kelvin Zou, Laura Heckman, Lauren Gardiner, Margit Bowler, Maria Cordell, Meng Cao, Nicole Hay, Nilesh Shahdarpuri, Otto Godwin, Pranay Dighe, Pushyami Rachapudi, Ramsey Tantawi, Roman Frigg, Sam Davarnia, Sanskruti Shah, Saptarshi Guha, Sasha Sirovica, Shen Ma, Shuang Ma, Simon Wang, Sulgi Kim, Suma Jayaram, Vaishaal Shankar, Varsha Paidi, Vivek Kumar, Xin Wang, Xin Zheng, Walker Cheng, Yael Shrager, Yang Ye, Yasu Tanaka, Yihao Guo, Yunsong Meng, Zhaoping Luo, Ouyang Zhi, Alp Ayyar, Alvin Wan, Andrew D. Walkingshaw, Tzu-Hsiang Lin, Arsalan Farooq, Brent Ramerth, Colorado Reed, Chris Bartels, Chris Chaney, David Rizati, Eric Liang Yang, Erin Feldman, Gabriel Hochstrasser, Guillaume Seguin, Irina Belousova, Joris Pelemans, Karen Yang, Keivan Alizadeh Vahid, Liangliang Cao, Mahyar Najibi, Marco Zuliani, Max Horton, Minsik Cho, Nikhil Bhendawade, Patrick Dong, Piotr Maj, Pulkit Agrawal, Qi Shan, Qichen Fu, Regan Poston, Sam Xu, Shuangning Liu, Sushma Rao, Tashweena Heeraman, Thomas Merth, Uday Rayala, Victor Cui, Vivek Rangarajan Sridhar, Wencong Zhang, Wenqi Zhang, Wentao Wu, Xingyu Zhou, Xinwen Liu, Yang Zhao, Yin Xia, Zhile Ren, and Zhongzheng Ren. Apple intelligence foundation language models. *ArXiv*, abs/2407.21075, 2024. URL <https://api.semanticscholar.org/CorpusID:271546289>.

- Alex Henry, Prudhvi Raj Dachapally, Shubham Vivek Pawar, and Yuxuan Chen. Query-key normalization for transformers. In *Findings*, 2020. URL <https://api.semanticscholar.org/CorpusID:222272447>.
- Huiqiang Jiang, Yucheng Li, Chengruidong Zhang, Qianhui Wu, Xufang Luo, Surin Ahn, Zhenhua Han, Amir H. Abdi, Dongsheng Li, Chin-Yew Lin, Yuqing Yang, and Lili Qiu. Minference 1.0: Accelerating pre-filling for long-context llms via dynamic sparse attention. *ArXiv*, abs/2407.02490, 2024. URL <https://api.semanticscholar.org/CorpusID:270877928>.
- Mandar Joshi, Eunsol Choi, Daniel S. Weld, and Luke Zettlemoyer. Triviaqa: A large scale distantly supervised challenge dataset for reading comprehension. *ArXiv*, abs/1705.03551, 2017. URL <https://api.semanticscholar.org/CorpusID:26501419>.
- Hao Kang, Qingru Zhang, Souvik Kundu, Geonhwa Jeong, Zaoxing Liu, Tushar Krishna, and Tuo Zhao. Gear: An efficient kv cache compression recipe for near-lossless generative inference of llm. *ArXiv*, abs/2403.05527, 2024. URL <https://api.semanticscholar.org/CorpusID:268297231>.
- Jared Kaplan, Sam McCandlish, Tom Henighan, Tom B. Brown, Benjamin Chess, Rewon Child, Scott Gray, Alec Radford, Jeff Wu, and Dario Amodei. Scaling laws for neural language models. *ArXiv*, abs/2001.08361, 2020. URL <https://api.semanticscholar.org/CorpusID:210861095>.
- Denis Kocetkov, Raymond Li, Loubna Ben Allal, Jia Li, Chenghao Mou, Carlos Muñoz Ferrandis, Yacine Jernite, Margaret Mitchell, Sean Hughes, Thomas Wolf, Dzmitry Bahdanau, Leandro von Werra, and Harm de Vries. The stack: 3 tb of permissively licensed source code. *ArXiv*, abs/2211.15533, 2022. URL <https://api.semanticscholar.org/CorpusID:254044610>.
- Yuhong Li, Yingbing Huang, Bowen Yang, Bharat Venkitesh, Acyr F. Locatelli, Hanchen Ye, Tianle Cai, Patrick Lewis, and Deming Chen. Snapkv: Llm knows what you are looking for before generation. *ArXiv*, abs/2404.14469, 2024. URL <https://api.semanticscholar.org/CorpusID:269303164>.
- Ji Lin, Jiaming Tang, Haotian Tang, Shang Yang, Xingyu Dang, and Song Han. Awq: Activation-aware weight quantization for on-device llm compression and acceleration. In *Conference on Machine Learning and Systems*, 2023. URL <https://api.semanticscholar.org/CorpusID:258999941>.
- Yuhan Liu, Han-Chiang Li, Kuntai Du, Jiayi Yao, Yihua Cheng, Qizheng Zhang, Yuyang Huang, Shan Lu, Michael Maire, Henry Hoffmann, Ari Holtzman, Ganesh Ananthanarayanan, and Junchen Jiang. Cachegen: Fast context loading for language model applications. *ArXiv*, abs/2310.07240, 2023. URL <https://api.semanticscholar.org/CorpusID:263834986>.
- Zirui Liu, Jiayi Yuan, Hongye Jin, Shaochen Zhong, Zhaozhuo Xu, Vladimir Braverman, Beidi Chen, and Xia Hu. Kivi: A tuning-free asymmetric 2bit quantization for kv cache. *ArXiv*, abs/2402.02750, 2024. URL <https://api.semanticscholar.org/CorpusID:267413049>.
- Junlin Lv, Yuan Feng, Xike Xie, Xin Jia, Qirong Peng, and Guiming Xie. Critiprefill: A segment-wise criticality-based approach for prefilling acceleration in llms. 2024. URL <https://api.semanticscholar.org/CorpusID:272753560>.
- Xinyin Ma, Gongfan Fang, and Xinchao Wang. Llm-pruner: On the structural pruning of large language models. *ArXiv*, abs/2305.11627, 2023. URL <https://api.semanticscholar.org/CorpusID:258823276>.
- Sachin Mehta, Mohammad Hossein Sekhavat, Qingqing Cao, Maxwell Horton, Yanzi Jin, Chenfan Sun, Iman Mirzadeh, Mahyar Najibi, Dmitry Belenko, Peter Zatloukal, and Mohammad Rastegari. Openelm: An efficient language model family with open training and inference framework. *ArXiv*, abs/2404.14619, 2024. URL <https://api.semanticscholar.org/CorpusID:269302585>.

- Guilherme Penedo, Quentin Malartic, Daniel Hesslow, Ruxandra-Aimée Cojocaru, Alessandro Cappelli, Hamza Alobeidli, Baptiste Pannier, Ebtesam Almazrouei, and Julien Launay. The refinedweb dataset for falcon llm: Outperforming curated corpora with web data, and web data only. *ArXiv*, abs/2306.01116, 2023. URL <https://api.semanticscholar.org/CorpusID:259063761>.
- Wenqi Shao, Mengzhao Chen, Zhaoyang Zhang, Peng Xu, Lirui Zhao, Zhiqiang Li, Kaipeng Zhang, Peng Gao, Yu Jiao Qiao, and Ping Luo. Omniquant: Omnidirectionally calibrated quantization for large language models. *ArXiv*, abs/2308.13137, 2023. URL <https://api.semanticscholar.org/CorpusID:261214575>.
- Jovan Stojkovic, Esha Choukse, Chaojie Zhang, Íñigo Goiri, and Josep Torrellas. Towards greener llms: Bringing energy-efficiency to the forefront of llm inference. *ArXiv*, abs/2403.20306, 2024. URL <https://api.semanticscholar.org/CorpusID:268793445>.
- Albert Tseng, Jerry Chee, Qingyao Sun, Volodymyr Kuleshov, and Christopher De Sa. Quip#: Even better llm quantization with hadamard incoherence and lattice codebooks. *ArXiv*, abs/2402.04396, 2024. URL <https://api.semanticscholar.org/CorpusID:267523209>.
- Ashish Vaswani, Noam M. Shazeer, Niki Parmar, Jakob Uszkoreit, Llion Jones, Aidan N. Gomez, Lukasz Kaiser, and Illia Polosukhin. Attention is all you need. In *Neural Information Processing Systems*, 2017. URL <https://api.semanticscholar.org/CorpusID:13756489>.
- Haoyi Wu and Kewei Tu. Layer-condensed kv cache for efficient inference of large language models. In *Annual Meeting of the Association for Computational Linguistics*, 2024. URL <https://api.semanticscholar.org/CorpusID:269899988>.
- Guangxuan Xiao, Yuandong Tian, Beidi Chen, Song Han, and Mike Lewis. Efficient streaming language models with attention sinks. *ArXiv*, abs/2309.17453, 2023. URL <https://api.semanticscholar.org/CorpusID:263310483>.
- Wenhan Xiong, Jingyu Liu, Igor Molybog, Hejia Zhang, Prajjwal Bhargava, Rui Hou, Louis Martin, Rashi Rungta, Karthik Abinav Sankararaman, Barlas Oğuz, Madian Khabza, Han Fang, Yashar Mehdad, Sharan Narang, Kshitiz Malik, Angela Fan, Shruti Bhosale, Sergey Edunov, Mike Lewis, Sinong Wang, and Hao Ma. Effective long-context scaling of foundation models. In *North American Chapter of the Association for Computational Linguistics*, 2023. URL <https://api.semanticscholar.org/CorpusID:263134982>.
- Zhewei Yao, Xiaoxia Wu, Conglong Li, Connor Holmes, Minjia Zhang, Cheng Li, and Yuxiong He. Random-ltd: Random and layerwise token dropping brings efficient training for large-scale transformers. *ArXiv*, abs/2211.11586, 2022. URL <https://api.semanticscholar.org/CorpusID:253735208>.
- Peiyuan Zhang, Guangtao Zeng, Tianduo Wang, and Wei Lu. Tinyllama: An open-source small language model. *ArXiv*, abs/2401.02385, 2024. URL <https://api.semanticscholar.org/CorpusID:266755802>.
- Haizhong Zheng, Xiaoyan Bai, Beidi Chen, Fan Lai, and Atul Prakash. Learn to be efficient: Build structured sparsity in large language models. *ArXiv*, abs/2402.06126, 2024. URL <https://api.semanticscholar.org/CorpusID:267617253>.

| $\lambda_C$ | Acc          |
|-------------|--------------|
| 0           | 8.95         |
| 1/28        | <b>17.38</b> |
| 1           | 15.96        |

Table 1: Ablation on TriviaQA (1-shot) of our choice of consistency loss coefficient  $\lambda_C$  with OpenELM1.1B-KVP-LP-0.50.<sup>1</sup>

| Model            | Layers Retained From OpenELM1.1B   |
|------------------|--|
| OpenELM1.1B-0.75 | 0, 1, 2, 4, 5, 6, 8, 9, 10, 12, 13, 14, 16, 17, 18, 20, 21, 22, 24, 25, 26 |
| OpenELM1.1B-0.50 | 0, 2, 4, 6, 8, 10, 12, 14, 16, 18, 20, 22, 24, 26                          |
| OpenELM1.1B-0.25 | 0, 4, 8, 12, 16, 20, 24  |

(a) Specification of layer-pruned OpenELM 1.1B architectures.

| Model          | Layers Retained From OpenELM3B   |
|----------------|--|
| OpenELM3B-0.75 | 0, 1, 2, 4, 5, 6, 8, 9, 10, 12, 13, 14, 16, 17, 18, 20, 21, 22, 24, 25, 26, 28, 29, 30, 32, 33, 34 |
| OpenELM3B-0.50 | 0, 2, 4, 6, 8, 10, 12, 14, 16, 18, 20, 22, 24, 26, 28, 30, 32, 34                                  |
| OpenELM3B-0.25 | 0, 4, 8, 12, 16, 20, 24, 28, 32  |

(b) Specification of layer-pruned OpenELM 3B architectures.

Table 2: Specification of layer-pruned OpenELM architectures.

## A LOSS FUNCTION

Our training loss consists of three components: the base loss  $\mathcal{L}_B$ , the auxiliary loss  $\mathcal{L}_A$ , and the consistency loss  $\mathcal{L}_C$ . The **base loss**  $\mathcal{L}_B = \mathcal{C}_B(\mathcal{B}(\mathcal{I}), \mathcal{T})$  is the cross-entropy loss between the base model’s outputs and the ground-truth labels  $\mathcal{T}$ . This loss helps ensure that the predicted KV cache is compatible with the base model. The **auxiliary loss**  $\mathcal{L}_A = \mathcal{C}_A(\mathcal{A}(\mathcal{I}), \mathcal{T})$  is the cross-entropy loss between the auxiliary model’s outputs and the ground-truth labels. We find that  $\mathcal{L}_A$  slightly improves the convergence of the training. The **consistency loss**  $\mathcal{L}_C = \mathbb{L}_1(\mathcal{K}\hat{\mathcal{V}}_B, \mathcal{K}\mathcal{V}_B)$  is used to align the predicted KV caches with the base model’s KV caches. The consistency loss is necessary to ensure that the predicted KV cache is compatible with the base model. To illustrate this point, we present an ablation in Table 1 showing a model trained with the consistency loss coefficient set to 0 ( $\lambda_C = 0$ ). Without the consistency loss, the predicted KV cache performs poorly.

Our final loss is a simple weighted sum of the individual losses:

$$\mathcal{L}(\mathcal{B}(\mathcal{I}), \mathcal{A}(\mathcal{I}), \mathcal{T}, \mathcal{K}\hat{\mathcal{V}}_B, \mathcal{K}\mathcal{V}_B) = \lambda_B \mathcal{L}_B + \lambda_A \mathcal{L}_A + \lambda_C \mathcal{L}_C \quad (1)$$

$$= \lambda_B \mathcal{C}_A(\mathcal{B}(\mathcal{I}), \mathcal{T}) + \lambda_A \mathcal{C}_A(\mathcal{A}(\mathcal{I}), \mathcal{T}) + \lambda_C \mathbb{L}_1(\mathcal{K}\hat{\mathcal{V}}_B, \mathcal{K}\mathcal{V}_B) \quad (2)$$

We found that the loss terms  $\mathcal{L}_B$  and  $\mathcal{L}_A$  were balanced by simply setting  $\lambda_B = \lambda_A = 1$ . To choose  $\lambda_C$ , we perform an ablation between summing the loss across layers ( $\lambda_C = 1$ ) and averaging the loss across layers ( $\lambda_C = 1/n_B$ ) in Table 1. We found that  $\lambda_C = 1/n_B$  performed better.

## B LAYER-PRUNED ARCHITECTURES

We provide details of our layer-pruned architectures here. Each architecture is defined by pruning layers at regular intervals from an existing OpenELM architecture. We specify the retained layers in Table 2.

## C ADDITIONAL ARCHITECTURAL DETAILS

### C.1 PREDICTOR NETWORKS

Here we formally describe the Predictor networks introduced in Section 3.2.

<sup>1</sup>Results differ slightly from other tables, as training hyperparameters were not finalized during this ablation.

| Model              | Aux        | $j_0$ | $j_1$ | $j_2$ | $j_3$ | $j_4$ | $j_5$ | $j_6$ | $j_7$ | $j_8$ | $j_9$ | $j_{10}$ | $j_{11}$ | $j_{12}$ | $j_{13}$ | $j_{14}$ | $j_{15}$ | $j_{16}$ | $j_{17}$ | $j_{18}$ | $j_{19}$ | $j_{20}$ | $j_{21}$ | $j_{22}$ | $j_{23}$ | $j_{24}$ | $j_{25}$ | $j_{26}$ | $j_{27}$ |
|--------------------|------------|-------|-------|-------|-------|-------|-------|-------|-------|-------|-------|----------|----------|----------|----------|----------|----------|----------|----------|----------|----------|----------|----------|----------|----------|----------|----------|----------|----------|
| OE1.1B-KVP-C-450M  | OE450M     | 0     | 0     | 1     | 1     | 2     | 3     | 3     | 4     | 4     | 5     | 5        | 6        | 6        | 7        | 7        | 8        | 9        | 10       | 11       | 12       | 13       | 14       | 15       | 16       | 17       | 18       | 19       |          |
| OE1.1B-KVP-C-270M  | OE270M     | 0     | 0     | 1     | 1     | 2     | 2     | 3     | 3     | 4     | 4     | 5        | 5        | 6        | 6        | 7        | 7        | 8        | 8        | 9        | 9        | 10       | 10       | 11       | 11       | 12       | 13       | 14       | 15       |
| OE1.1B-KVP-LP-0.75 | OE-LP-0.75 | 0     | 1     | 2     | 2     | 3     | 4     | 5     | 5     | 6     | 7     | 8        | 8        | 9        | 10       | 11       | 11       | 12       | 13       | 14       | 14       | 15       | 16       | 17       | 17       | 18       | 19       | 20       | 20       |
| OE1.1B-KVP-LP-0.50 | OE-LP-0.50 | 0     | 0     | 1     | 1     | 2     | 2     | 3     | 3     | 4     | 4     | 5        | 5        | 6        | 6        | 7        | 7        | 8        | 8        | 9        | 9        | 10       | 10       | 11       | 11       | 12       | 12       | 13       | 13       |
| OE1.1B-KVP-LP-0.25 | OE-LP-0.25 | 0     | 0     | 0     | 0     | 1     | 1     | 1     | 1     | 1     | 2     | 2        | 2        | 2        | 3        | 3        | 3        | 3        | 4        | 4        | 4        | 4        | 5        | 5        | 5        | 5        | 6        | 6        | 6        |

(a) KV Prediction models using a base model of OpenELM 1.1B.

| Model            | Aux        | $j_0$ | $j_1$ | $j_2$ | $j_3$ | $j_4$ | $j_5$ | $j_6$ | $j_7$ | $j_8$ | $j_9$ | $j_{10}$ | $j_{11}$ | $j_{12}$ | $j_{13}$ | $j_{14}$ | $j_{15}$ | $j_{16}$ | $j_{17}$ | $j_{18}$ | $j_{19}$ | $j_{20}$ | $j_{21}$ | $j_{22}$ | $j_{23}$ | $j_{24}$ | $j_{25}$ | $j_{26}$ | $j_{27}$ |    |
|------------------|------------|-------|-------|-------|-------|-------|-------|-------|-------|-------|-------|----------|----------|----------|----------|----------|----------|----------|----------|----------|----------|----------|----------|----------|----------|----------|----------|----------|----------|----|
| OE3B-KVP-C-1.1B  | OE1.1B     | 0     | 0     | 1     | 1     | 2     | 2     | 3     | 3     | 4     | 4     | 5        | 5        | 6        | 6        | 7        | 7        | 8        | 9        | 10       | 11       | 12       | 13       | 14       | 15       | 16       | 17       | 18       | 19       | 20 |
| OE3B-KVP-C-450M  | OE450M     | 0     | 0     | 1     | 1     | 2     | 2     | 3     | 3     | 4     | 4     | 5        | 5        | 6        | 6        | 7        | 7        | 8        | 8        | 9        | 9        | 10       | 10       | 11       | 11       | 12       | 12       | 13       | 14       | 15 |
| OE3B-KVP-C-270M  | OE270M     | 0     | 0     | 0     | 1     | 1     | 1     | 2     | 2     | 2     | 3     | 3        | 3        | 4        | 4        | 5        | 5        | 6        | 6        | 7        | 7        | 8        | 8        | 9        | 9        | 10       | 10       | 11       | 11       | 12 |
| OE3B-KVP-LP-0.75 | OE-LP-0.75 | 0     | 1     | 2     | 2     | 3     | 4     | 5     | 5     | 6     | 7     | 8        | 8        | 9        | 10       | 11       | 11       | 12       | 13       | 14       | 14       | 15       | 16       | 17       | 17       | 18       | 19       | 20       | 21       | 22 |
| OE3B-KVP-LP-0.50 | OE-LP-0.50 | 0     | 0     | 1     | 1     | 2     | 2     | 3     | 3     | 4     | 4     | 5        | 5        | 6        | 6        | 7        | 7        | 8        | 8        | 9        | 9        | 10       | 10       | 11       | 11       | 12       | 12       | 13       | 13       | 14 |
| OE3B-KVP-LP-0.25 | OE-LP-0.25 | 0     | 0     | 0     | 0     | 1     | 1     | 1     | 1     | 2     | 2     | 2        | 2        | 3        | 3        | 3        | 3        | 4        | 4        | 4        | 4        | 5        | 5        | 5        | 5        | 6        | 6        | 6        | 6        | 7  |

(b) KV Prediction models using a base model of OpenELM 3B.

Table 3: KV Prediction models. Each model is specified by a base network, an auxiliary network, and the mapping of input auxiliary layers  $j_i$  to base layers  $i$ . (Table 3a): models using a base network of OpenELM 1.1B. (Table 3b): models using a base network of OpenELM 3B.

When choosing the auxiliary KV cache layer  $j_i$  to predict the base KV cache layer  $i$ , we build on top of the observation in Brandon et al. (2024) that neighboring transformer layers will have KV caches that are more similar than distant layers. Thus, we use the first layer of  $\mathcal{KV}_A$  as input to predict the first several layers of  $\mathcal{KV}_B$ , and the second layer of  $\mathcal{KV}_A$  as input to predict the next several layers of  $\mathcal{KV}_B$ , and so forth. When  $n_A$  does not divide evenly into  $n_B$ , we perform rounding.

More formally, we need to choose which layer of the auxiliary cache to use to predict each layer of the base cache. To do this, we define a mapping from auxiliary cache layers  $j$  to base cache layers  $i$ . Let  $n_B$  be the number of transformer layers in the base network, and  $n_A$  be the number of transformer layers in the auxiliary network. For each  $i \in [0, \dots, n_B - 1]$ , let  $j_i \in [0, \dots, n_A - 1]$  denote the  $j_i$ th layer of the auxiliary cache  $\mathcal{KV}_{A,j_i}$ . We will use  $\mathcal{KV}_{A,j_i}$  as input to a linear function to predict the layer of the base cache  $\mathcal{KV}_{B,i}$ .

Now that we have defined our mapping  $j_i$ , we define our set of linear functions. Our linear functions are defined as  $\mathcal{F}_i(\mathcal{KV}_{A,j_i}) : \mathcal{R}^{d_{\mathcal{KV}_{A,j_i}}} \rightarrow \mathcal{R}^{d_{\mathcal{KV}_{B,i}}}$ , where  $d_{\mathcal{KV}_{A,j_i}}$ ,  $d_{\mathcal{KV}_{B,i}}$  are the feature dimensions of the auxiliary and base KV caches at layers  $j_i$  and  $i$ , respectively. We use these linear functions to compute each layer of the base KV cache,  $\mathcal{KV}_{B,i} = \mathcal{F}_i(\mathcal{KV}_{A,j_i})$ . Once each layer  $\mathcal{KV}_{B,i}$  is predicted, we concatenate them to produce  $\mathcal{KV}_B$ .

## C.2 KV PREDICTION MODELS

Our KV Prediction models are specified by a base network, an auxiliary network, and the mapping of input auxiliary layers  $j_i$  used to predict base KV cache layer  $i$ . Full details are presented in Table 3.

## D ADDITIONAL TRAINING DETAILS

To train our models, we reload the base and auxiliary model weights from pretrained OpenELM models (in the case of KVP-LP experiments, we only reload the unpruned layers into the auxiliary model). We follow the training hyperparameters of OpenELM, training on RefinedWeb (Penedo et al., 2023), ArXiv (Clement et al., 2019), and Wikipedia (Foundation, 2024). For code completion experiments, we train on The Stack (Kocetkov et al., 2022).

We shorten the training regime to 70k iterations on 64 H100 GPUs at a token length of 2048 and a batch size of 16. For code completion experiments, our training setup is the same, but we instead train on The Stack (Kocetkov et al., 2022) and divide the learning rate by 10. A complete list of configs appears in our code release for reproducibility.

## E ADDITIONAL BASELINE DETAILS

Here, we describe our token pruning baselines in more detail. Our implementations follow Fu et al. (2024).

| Model              | FLOPs Reduction (Rel) $\uparrow$ | TTFT (s) $\downarrow$ | TTFT Reduction (Rel) $\uparrow$ | TQA $\uparrow$ | TQA (Rel) $\uparrow$ |
|--------------------|----------------------------------|-----------------------|---------------------------------|----------------|----------------------|
| OE1.1B             | 1.00                             | 5.59                  | 1.00                            | 23.57          | 1.00                 |
| OE450M             | 2.36                             | 2.58                  | 2.17                            | 10.97          | 0.41                 |
| OE270M             | 3.98                             | 1.67                  | 3.34                            | 7.04           | 0.27                 |
| OE1.1B-LP-0.75     | 1.34                             | 4.08                  | 1.37                            | 15.04          | 0.57                 |
| OE1.1B-LP-0.50     | 1.93                             | 2.78                  | 2.01                            | 10.13          | 0.38                 |
| OE1.1B-LP-0.25     | 3.60                             | 1.46                  | 3.82                            | 4.21           | 0.16                 |
| OE1.1B-KVP-C-450M  | 2.36                             | 3.17                  | 1.76                            | 16.09          | 0.61                 |
| OE1.1B-KVP-C-270M  | 3.98                             | 2.24                  | 2.50                            | 11.71          | 0.44                 |
| OE1.1B-KVP-LP-0.75 | 1.34                             | 4.63                  | 1.21                            | 20.73          | 0.78                 |
| OE1.1B-KVP-LP-0.50 | 1.93                             | 3.33                  | 1.68                            | 17.59          | 0.66                 |
| OE1.1B-KVP-LP-0.25 | 3.60                             | 2.05                  | 2.73                            | 10.38          | 0.39                 |
| RP-0.75            | 1.33                             | 4.31                  | 1.30                            | 2.61           | 0.10                 |
| RP-0.50            | 2.00                             | 2.94                  | 1.90                            | 0.08           | 0.00                 |
| RP-0.25            | 4.00                             | 4.31                  | 1.30                            | 0.01           | 0.00                 |
| SP-0.50            | 1.33                             | 3.73                  | 1.50                            | 4.29           | 0.16                 |
| SP-0.25            | 2.00                             | 2.51                  | 2.22                            | 0.38           | 0.01                 |
| L0.75-0.75         | 1.21                             | 4.47                  | 1.25                            | 19.33          | 0.73                 |
| L0.75-0.50         | 1.38                             | 4.09                  | 1.37                            | 18.78          | 0.71                 |
| L0.75-0.25         | 1.60                             | 3.69                  | 1.51                            | 17.89          | 0.67                 |
| L0.75-0.10         | 1.89                             | 3.18                  | 1.76                            | 14.63          | 0.55                 |
| L0.75-0.05         | 1.83                             | 3.24                  | 1.72                            | 15.70          | 0.59                 |
| L0.75-0.01         | 1.77                             | 3.36                  | 1.66                            | 16.25          | 0.61                 |
| L0.50-0.50         | 1.54                             | 3.38                  | 1.65                            | 8.69           | 0.33                 |
| L0.50-0.25         | 1.82                             | 3.19                  | 1.75                            | 7.36           | 0.28                 |
| L0.50-0.10         | 2.04                             | 2.79                  | 2.00                            | 6.21           | 0.23                 |
| L0.50-0.05         | 2.13                             | 2.68                  | 2.09                            | 5.56           | 0.21                 |
| L0.50-0.01         | 2.20                             | 2.65                  | 2.11                            | 5.06           | 0.19                 |

Table 4: Relative FLOPs, runtime and accuracy values for OpenELM 1.1B on TriviaQA. Values are used to produce Fig. 3 (Left) and Fig. 5a.

Our **RP** baseline consists of randomly pruning tokens from the input, sweeping across token retention ratios of [0.25, 0.50, 0.75]. Our **SP** baseline consists of probing the first 25% of network layers to obtain attention weights, then pruning tokens that have low attention scores and rerunning on the pruned tokens. We use token retention rates of [0.25, 0.50], omitting the higher retention rate of 0.75 since the overhead of processing 25% of the query with the unpruned input means that lower retention ratios are needed to obtain a similar speedup to random pruning. Our **L** baseline consists of LazyLLM (Fu et al., 2024). LazyLLM prunes at progressively higher rates through the network, from an initial higher retention rate (or low pruning rate) to a final lower retention rate (or higher pruning rate). We adopt the standard configuration suggested by the authors of beginning pruning 30% of the way into the network and ending pruning 90% of the way into the network. For **L0.75**, our beginning retention rate (which is active 30% of the way into the network) is 75%, and we sweep across ending retention rates of [0.75, 0.50, 0.25, 0.10, 0.05, 0.01]. For **L0.50**, our beginning retention rate is 0.50, and we sweep across end retention rates [0.50, 0.25, 0.10, 0.05, 0.01].

## F ACCURACY VALUES

We give values used to produce plots. In Table 4, we give accuracies and timing results for OpenELM 1.1B on TriviaQA. In Table 5, we give accuracies for OpenELM 3B on TriviaQA. In Table 6, we give accuracies for OpenELM 1.1B on HumanEval.

| <b>Model</b>     | <b>FLOPs Reduction (Rel) ↑</b> | <b>TQA ↑</b> | <b>TQA (Rel) ↑</b> |
|------------------|--------------------------------|--------------|--------------------|
| OE3B             | 1.00                           | 40.87        | 1.00               |
| OE1.1B           | 2.81                           | 23.57        | 0.58               |
| OE450M           | 6.64                           | 10.97        | 0.27               |
| OE270M           | 11.18                          | 7.04         | 0.17               |
| OE3B-LP-0.75     | 1.34                           | 33.31        | 0.81               |
| OE3B-LP-0.50     | 1.97                           | 23.94        | 0.59               |
| OE3B-LP-0.25     | 3.84                           | 9.43         | 0.23               |
| OE3B-KVP-C-1.1B  | 2.81                           | 28.83        | 0.71               |
| OE3B-KVP-C-450M  | 6.64                           | 15.64        | 0.38               |
| OE3B-KVP-C-270M  | 11.18                          | 16.70        | 0.41               |
| OE3B-KVP-LP-0.75 | 1.34                           | 35.43        | 0.87               |
| OE3B-KVP-LP-0.50 | 1.97                           | 30.41        | 0.74               |
| OE3B-KVP-LP-0.25 | 3.84                           | 13.11        | 0.32               |
| RP 0.75          | 1.33                           | 5.09         | 0.12               |
| RP 0.50          | 2.00                           | 0.22         | 0.01               |
| RP0.25           | 4.00                           | 0.02         | 0.00               |
| SP 0.50          | 1.33                           | 9.45         | 0.23               |
| SP 0.25          | 2.00                           | 1.04         | 0.03               |
| L0.75-0.75       | 1.21                           | 19.90        | 0.49               |
| L0.75-0.50       | 1.38                           | 19.93        | 0.49               |
| L0.75-0.25       | 1.60                           | 19.68        | 0.48               |
| L0.75-0.10       | 1.89                           | 18.35        | 0.45               |
| L0.75-0.05       | 1.83                           | 18.58        | 0.45               |
| L0.75-0.01       | 1.77                           | 18.95        | 0.46               |
| L0.50-0.50       | 1.54                           | 4.04         | 0.10               |
| L0.50-0.25       | 1.82                           | 3.95         | 0.10               |
| L0.50-0.10       | 2.04                           | 3.81         | 0.09               |
| L0.50-0.05       | 2.13                           | 3.72         | 0.09               |
| L0.50-0.01       | 2.20                           | 3.66         | 0.09               |

Table 5: Relative FLOPs and accuracy values of OpenELM 3B on TriviaQA. Values are used to produce Fig. 3 (Right).

| Model              | FLOPs Reduction (Rel) $\uparrow$ | Pass@1 $\uparrow$ | Pass@1 (Rel) $\uparrow$ | Pass@10 $\uparrow$ | Pass@10 (Rel) $\uparrow$ |
|--------------------|----------------------------------|-------------------|-------------------------|--------------------|--------------------------|
| OE1.1B             | 1.00                             | 15.79             | 1.00                    | 23.07              | 1.00                     |
| OE450M             | 2.36                             | 8.85              | 0.56                    | 14.33              | 0.62                     |
| OE270M             | 3.98                             | 7.41              | 0.47                    | 11.51              | 0.50                     |
| OE1.1B-LP-0.75     | 1.34                             | 1.30              | 0.72                    | 17.85              | 0.77                     |
| OE1.1B-LP-0.50     | 1.93                             | 10.46             | 0.66                    | 14.36              | 0.62                     |
| OE1.1B-LP-0.25     | 3.60                             | 3.37              | 0.21                    | 6.94               | 0.30                     |
| OE1.1B-KVP-C-450M  | 2.36                             | 10.12             | 0.64                    | 14.37              | 0.62                     |
| OE1.1B-KVP-C-270M  | 3.98                             | 7.20              | 0.46                    | 11.68              | 0.51                     |
| OE1.1B-KVP-LP-0.75 | 1.34                             | 13.82             | 0.88                    | 19.83              | 0.86                     |
| OE1.1B-KVP-LP-0.50 | 1.93                             | 11.51             | 0.73                    | 19.03              | 0.82                     |
| OE1.1B-KVP-LP-0.25 | 3.60                             | 6.24              | 0.39                    | 10.73              | 0.47                     |
| RP-0.75            | 1.33                             | 1.90              | 0.12                    | 6.71               | 0.29                     |
| RP-0.50            | 2.00                             | 0.08              | 0.01                    | 0.61               | 0.03                     |
| RP-0.25            | 4.00                             | 0.00              | 0.00                    | 0.00               | 0.00                     |
| SP-0.50            | 1.33                             | 0.01              | 0.00                    | 0.06               | 0.00                     |
| SP-0.25            | 2.00                             | 0.00              | 0.00                    | 0.00               | 0.00                     |
| L0.75-0.75         | 1.21                             | 9.81              | 0.62                    | 15.43              | 0.67                     |
| L0.75-0.50         | 1.38                             | 10.46             | 0.66                    | 15.85              | 0.69                     |
| L0.75-0.25         | 1.60                             | 10.97             | 0.69                    | 16.08              | 0.70                     |
| L0.75-0.10         | 1.77                             | 10.63             | 0.67                    | 15.00              | 0.65                     |
| L0.75-0.05         | 1.83                             | 10.56             | 0.67                    | 14.62              | 0.63                     |
| L0.75-0.01         | 1.89                             | 6.44              | 0.41                    | 12.46              | 0.54                     |
| L0.50-0.50         | 1.54                             | 2.63              | 0.17                    | 5.71               | 0.25                     |
| L0.50-0.25         | 1.82                             | 2.50              | 0.16                    | 5.37               | 0.23                     |
| L0.50-0.10         | 2.04                             | 1.97              | 0.12                    | 4.91               | 0.21                     |
| L0.50-0.05         | 2.13                             | 2.19              | 0.14                    | 5.77               | 0.25                     |
| L0.50-0.01         | 2.20                             | 0.77              | 0.05                    | 3.42               | 0.15                     |

Table 6: Relative FLOPs and accuracy values of OpenELM 1.1B on HumanEval. Values are used to produce Fig. 4.

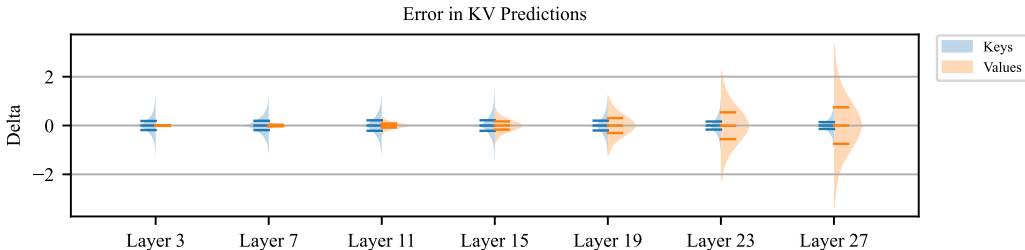


Figure 6: Distribution of the delta between KV cache predictions and targets in 7 different layers of OpenELM-1.1B-KVP-C-450M. The distributions of deltas for keys (blue) and values (orange) are shown separately.

| Model              | arc-c        | arc-e        | boolq        | hellaswag    | piqa         | sciq         | winogrande   | Avg          | TTFT Reduction |
|--------------------|--------------|--------------|--------------|--------------|--------------|--------------|--------------|--------------|----------------|
| OE 1.1B            | 32.34        | 55.43        | 63.58        | 64.81        | 75.57        | 90.60        | 61.72        | 63.43        | 1.0            |
| OE1.1B-KVP-LP-0.75 | <b>30.97</b> | <b>54.42</b> | <b>59.79</b> | <b>62.91</b> | <b>74.92</b> | <b>90.40</b> | <b>62.04</b> | <b>62.21</b> | 1.34           |
| OE 1.1B-0.75       | 29.52        | 51.81        | 57.52        | 58.38        | 73.88        | 87.70        | 60.46        | 59.90        | 1.34           |
| OE1.1B-KVP-LP-0.50 | <b>30.80</b> | <b>53.75</b> | 58.17        | <b>60.35</b> | <b>74.32</b> | <b>88.90</b> | <b>58.96</b> | <b>60.75</b> | 1.93           |
| OE 1.1B-0.50       | 26.28        | 48.15        | <b>59.79</b> | 53.74        | 71.33        | 86.10        | 57.46        | 57.55        | 1.93           |
| OE1.1B-KVP-C-450M  | <b>29.01</b> | <b>52.53</b> | <b>57.95</b> | <b>59.20</b> | <b>73.01</b> | <b>88.00</b> | <b>59.43</b> | <b>59.88</b> | 2.36           |
| OE 450M            | 27.56        | 48.06        | 55.78        | 53.97        | 72.31        | 87.20        | 58.01        | 57.56        | 2.36           |
| OE1.1B-KVP-LP-0.25 | <b>27.65</b> | <b>46.68</b> | 56.88        | <b>54.34</b> | <b>72.09</b> | <b>85.00</b> | <b>55.33</b> | <b>56.85</b> | 3.59           |
| OE 1.1B-0.25       | 24.15        | 41.84        | <b>60.49</b> | 43.08        | 68.61        | 82.60        | 52.41        | 53.31        | 3.59           |
| OE1.1B-KVP-C-270M  | <b>28.41</b> | <b>48.70</b> | 53.67        | <b>55.35</b> | <b>71.98</b> | <b>87.30</b> | <b>57.38</b> | <b>57.54</b> | 3.98           |
| OE 270M            | 26.45        | 45.08        | <b>53.98</b> | 46.71        | 69.75        | 84.70        | 53.91        | 54.37        | 3.98           |

Table 7: Comparison of OpenELM 1.1B KV Prediction models with using only the auxiliary model or only the base model for Multiple-Choice Question Answering. We de-emphasize “TTFT Reduction” since the concept doesn’t apply to multiple-choice question-answering evaluations.

## G TIMING EXPERIMENTS DETAILS

We measure the reduction in TTFT on an M2 Pro CPU (EveryMac, 2024) with 32GB of RAM using the average query length of TriviaQA 1-shot (59 tokens) and a batch size of 64.

For Fig. 5b, we set the batch size to 8 and sweep across prompt lengths.

| Model             | arc-c        | arc-e        | boolq        | hellaswag    | piqa         | sciq         | winogrande   | Avg          | TTFT Reduction |
|-------------------|--------------|--------------|--------------|--------------|--------------|--------------|--------------|--------------|----------------|
| OE 3B             | 35.58        | 59.89        | 67.40        | 72.44        | 78.24        | 92.70        | 65.51        | 67.39        | 1.0            |
| OE3B-KVP-LP-0.75  | <b>34.04</b> | 57.28        | <b>66.73</b> | <b>69.94</b> | <b>77.58</b> | <b>92.00</b> | <b>63.30</b> | <b>65.84</b> | 1.34           |
| OE 3B-0.75        | 33.53        | <b>59.89</b> | 65.14        | 67.60        | 76.71        | <b>92.00</b> | 62.75        | 65.37        | 1.34           |
| OE3B-KVP-L-0.50   | <b>33.87</b> | <b>56.65</b> | <b>64.50</b> | <b>67.06</b> | <b>76.77</b> | <b>90.00</b> | 59.67        | <b>64.07</b> | 1.97           |
| OE 3B-0.50        | 31.06        | 54.67        | 63.36        | 62.43        | 75.95        | 89.50        | <b>60.54</b> | 62.50        | 1.97           |
| OE3B-KVP-C-OE1.1B | <b>33.96</b> | <b>57.66</b> | <b>64.50</b> | <b>66.66</b> | <b>76.71</b> | 90.30        | 61.64        | <b>64.49</b> | 2.81           |
| OE1.1B            | 32.34        | 55.43        | 63.58        | 64.81        | 75.57        | <b>90.60</b> | <b>61.72</b> | 63.43        | 2.81           |
| OE3B-KVP-LP-0.25  | <b>29.27</b> | <b>51.39</b> | <b>62.63</b> | <b>58.87</b> | <b>74.59</b> | 85.30        | 56.27        | <b>59.76</b> | 3.84           |
| OE3B-0.25         | 26.88        | 47.10        | 59.69        | 49.89        | 71.33        | <b>86.00</b> | <b>58.56</b> | 57.06        | 3.84           |
| OE3B-KVP-LP-450M  | <b>30.97</b> | <b>54.00</b> | <b>62.84</b> | <b>61.94</b> | <b>74.76</b> | <b>88.50</b> | 57.46        | <b>61.50</b> | 6.64           |
| OE450M            | 27.56        | 48.06        | 55.78        | 53.97        | 72.31        | 87.20        | <b>58.01</b> | 57.56        | 6.64           |
| OE3B-KVP-C-270M   | <b>29.27</b> | <b>49.87</b> | <b>59.48</b> | <b>59.09</b> | <b>73.50</b> | <b>87.50</b> | <b>56.35</b> | <b>59.30</b> | 11.18          |
| OE 270M           | 26.45        | 45.08        | 53.98        | 46.71        | 69.75        | 84.70        | 53.91        | 54.37        | 11.18          |

Table 8: Comparison of OpenELM 3B model variants on Multiple-Choice Question Answering. We de-emphasize “TTFT Reduction” since the concept of TTFT doesn’t apply to multiple-choice question-answering evaluations.

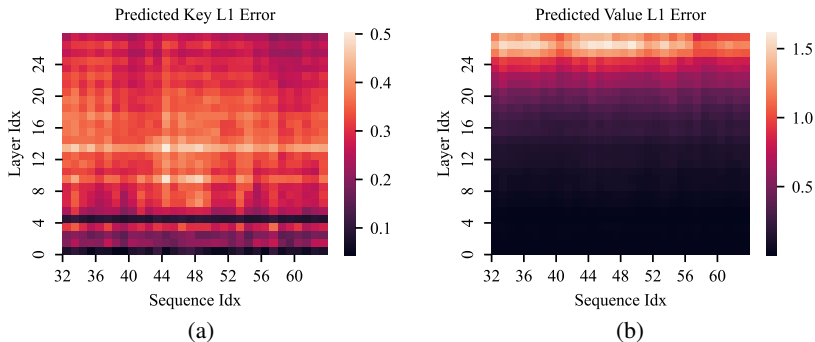


Figure 7: L1 error of predicted keys (Fig. 7a) and values (Fig. 7b) across the layer and sequence dimensions of OpenELM-1.1B-KVP-C-450M.

## H ADDITIONAL ANALYSIS

To better understand the performance of our KV cache prediction method, and to motivate future optimizations to improve performance, we analyze the quality of the KV cache predictions.

**L1 Error Across Sequences and Layers:** We analyze the distribution of the L1 loss across layers and sequence indexes in Fig. 7. The errors are relatively stable across sequence index, with a few outliers. Across layers, the magnitude of key error is stable due to OpenELM’s usage of key norm (Henry et al., 2020). Value error generally increases with depth due to propagation of errors.

**Multiple-Choice Question Answering:** We analyze the quality of KV cache predictions by running multiple-choice question answering (MCQA) evaluations using the predicted cache as the keys and values for the base model. Since these MCQA evaluations don’t produce output tokens, there is no notion of TTFT, and our method doesn’t provide a speedup. The purpose of these evaluations is to measure the consistency of the predicted KV cache with the base KV cache through accuracy retention on MCQA.

In Table 7, we present results for 7 MCQA tasks on OpenELM 1.1B and KV Prediction models. We directly compare each KV Prediction model to the results obtained by using only the auxiliary model. In all cases, the KV Prediction model obtains higher average accuracy. We present additional results on OpenELM 3B in Table 8.

**Density of Differences:** In Fig. 6, we analyze the distribution of the differences between the predicted KV cache and the target KV cache (e.g. similar to the  $\mathcal{L}_C$  introduced in Appendix A, but without the absolute value being computed). We pass a batch of data through our KV prediction model (to produce predictions  $\mathcal{K}\hat{\mathcal{V}}_B$ ) and through the base model (to produce targets  $\mathcal{K}\mathcal{V}_B$ ), and compute the delta between the predictions and targets at every layer.

We observe that the delta for keys is stable, ranging roughly from -1 to 1 and centered at 0 at all layers. This is due to the fact that OpenELM uses normalized keys, so the distribution of the deltas is relatively consistent. By contrast, the error in predicted values increases with network depth. The distribution remains centered at 0, indicating that our cache prediction method is unbiased.